Hindawi
Advances in Astronomy
Volume 2019, Article ID 4593092, 9 pages
https://doi.org/10.1155/2019/4593092

Research Article

Mass Transfer and Intrinsic Light Variability in the Contact Binary MT Cas

Haifeng Dai, Huiyu Yuan, and Yuangui Yang

School of Physics and Electronic Information/Information College, Huaibei Normal University, Huaibei 235000, China

Correspondence should be addressed to Yuangui Yang; yygcn@163.com

Received 12 November 2018; Accepted 19 March 2019; Published 4 April 2019

Academic Editor: Dean Hines

First CCD photometry for the contact binary MT Cas is performed in 2013 in December. The spectral type of F8V is determined from the low-precision spectrum observed on 2018 Oct 22. With Wilson-Devinney code, the photometric solutions are deduced from VR_c light curves (LCs) and AAVSO's and ASAS-SN's data, respectively. The results imply that MT Cas is a W-type weak-contact binary with a mass ratio of $q = 2.365(\pm0.005)$ and a fill-out factor of $f = 16.6(\pm1.2)\%$, respectively. The asymmetric LCs in 2013 are modeled by a dark spot on the more massive component. By analyzing the $(O-C)$ curve, it is discovered that the orbital period may be undergoing a secular increase at a rate of $dP/dt = 1.12(\pm0.09) \times 10^{-8}$d yr^{-1}, which may result from mass transfer from the less massive component to the more massive one. With mass transferring, MT Cas may evolve into a broken-contact configuration as predicted by TRO theory.

1. Introduction

W Ursae Majoris binary contains two components, which are embedded in a common envelope [1, 2]. Models for contact binary have been recently constructed by several investigators (e.g., see [3–5]). However, their evolutionary status still remains unclear because the spectra cannot be analyzed for abundances due to the extreme broadening and blending of spectral lines. Therefore, it is crucially important to observe contact binaries, which may provide some special phenomena and processes, such as magnetic activity [6], third body [7], angular momentum evolution [3], flare [8], and stellar coalescence [9]. It is helpful for us to understand their formation, structure, and evolution of contact binaries.

MT Cas (=SV∗ SON 4671) was found by Götz & Wenzel [10] as a W UMa-type eclipsing binary. Its visual magnitude is 13.3 mag, and the depths of both eclipses are 0.83 mag and 0.72 mag, respectively [11]. Hoffmann [12] photoelectrically observed this binary. Unfortunately, the *BV* light curves did not cover the complete period. Pribulla et al. [13] derived a linear ephemeris with a period of 0.31387775 days, which was updated to be 0.3138789 days [14]. Except for some photometric data performed by several amateur observers of AAVSO (https://www.aavso.org/data-download) and ASAS-SN database [15] (https://asas-sn.osu.edu/database/light_curves/335960), no additional observations for this binary have been presented up to now.

In this paper, the neglected binary MT Cas was studied photometrically and spectroscopically in Section 2. The orbital period variation is analyzed in Section 3, and three sets of light curves (i.e., VR_c LCs in 2013, AAVSO's LC, and ASAS-SN LC) are modeled in Section 4. In Section 5, we estimated the absolute parameters and discuss mass transfer between two components and its evolutionary status.

2. New Observations

2.1. Photometry. CCD photometry for MT Cas was first carried out at six nights of 2013, with the 85-cm telescope [16] at the Xinglong station (XLs) of National Astronomical Observatories of China (NAOC). The standard Johnson-Cousins UBVR_cI$_c$ systems were mounted onto this telescope. During the observation, VR_c files are used in order to provide the enough high time resolution. The image reductions are done by using the Image Reduction (IMRED) and Aperture Photometry (APPHOT) packages in the Image Reduction

Table 1: CCD photometric observations in V and R_c bands.

V band				R_c band			
HJD	Δm	HJD	Δm	HJD	Δm	HJD	Δm
2456629.9265	+0.066	2456632.9847	−0.273	2456629.9275	+0.269	2456632.9895	−0.076
2456629.9285	+0.106	2456632.9861	−0.280	2456629.9294	+0.322	2456632.9962	−0.091
2456629.9304	+0.133	2456632.9874	−0.273	2456629.9314	+0.349	2456632.9976	−0.113
2456629.9323	+0.176	2456632.9901	−0.289	2456629.9333	+0.384	2456632.9989	−0.099
2456629.9343	+0.225	2456632.9915	−0.300	2456629.9352	+0.413	2456633.0003	−0.116
.....							
2456632.9766	−0.235	2456636.0355	−0.077	2456632.9814	−0.057		
2456632.9780	−0.238	2456636.0373	−0.041	2456632.9827	−0.069		
2456632.9793	−0.263	2456636.0391	−0.041	2456632.9841	−0.069		
2456632.9807	−0.267	2456636.0409	+0.007	2456632.9854	−0.063		
2456632.9820	−0.270	2456636.0427	+0.065	2456632.9868	−0.081		
2456632.9834	−0.261			2456632.9881	−0.076		

Note. The entire table is available only on the online journal.

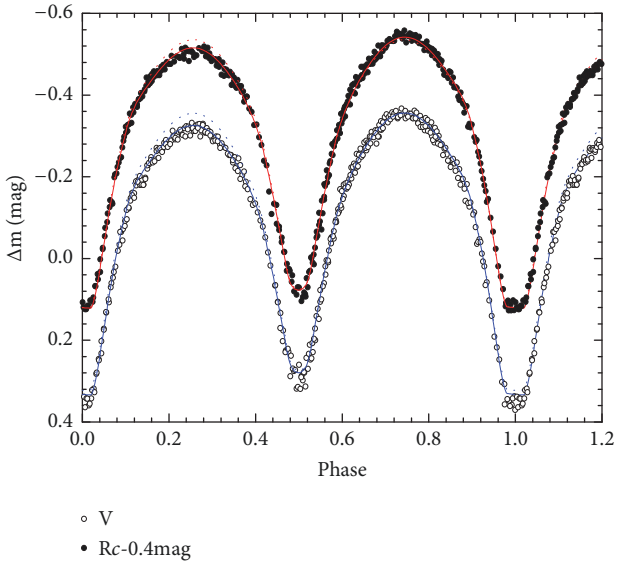

Figure 1: VR_c light curves of the contact binary MT Cas, which are observed in 2013 in December by using the 85-cm telescope. The dotted and solid lines are plotted by photometric solutions without or with a dark spot, respectively.

and Analysis Facility (IRAF) in a standard mode. Differential magnitudes were then determined by aperture photometry.

In the observing process, we chose TYC 3657-1637-1 (α_{J2000} = $00^h14^m59.^s4$ and δ_{J2000} = $+54^\circ39'53.''1$) and TYC 3657-1245-1 (α_{J2000} = $00^h14^m32.^s6$ and δ_{J2000} = $+54^\circ29'16.''1$) as the comparison and check stars, respectively. Typical exposure times are adopted to be 60s in V band and 50s in R_c band, respectively. In total, we obtained 383 and 373 images in V and R_c bands. The standard uncertainties are ±0.005 mag in V band and ±0.004 mag in R_c band. All individual observations (i.e., HJD and Δm) are listed in Table 1. The differential magnitudes *versus* orbital phases are displayed in Figure 1, where phases are computed by a period of $0.^d3138789$ (Kreiner et al. 2004). The VR_c LCs in 2013 imply that MT Cas is an UMa-type eclipsing binary, whose amplitudes of variable light are 0.69 mag and 0.66 mag in V and R_c bands, respectively. There exists an unequal height between both maxima, i.e., O'Connell effect [17, 18]. Max.II at phase 0.75 is brighter than Max.I at phase 0.25 up to 0.025 mag and 0.029 mag in V and R_c bands, respectively. This kind of stellar activity occurs on other W UMa-type binaries, such as VW Cep [19], DV CVn [20], V532 Mon [21], and BB Peg (Kalomeni et al. 2007), and DZ Psc [22].

2.2. Low-Precision Spectrum. The low-precision spectrum for MT Cas was obtained by using the *Yunnan Faint Object Spectrograph and Camera* (YFOSC), which is attached to the 2.4-m telescope at Lijiang station (LJs) of Yunnan Astronomical Observatory of China (YNAO) at UT 15:50:13 of 2018 October 22. During the observing process, we chose a 140-mm-length slit and a *Grism*-3 with a wavelength range from 3200 Å to 9200 Å [23]. The exposure time is 10 minutes. The phase of 0.98 almost corresponds to the observed middle time HJD 245414.1634. Reduction of the spectra was performed by using IRAF packages, including bias subtraction, flat-fielding, and cosmic-ray removal. Finally, the one-dimensional spectrum was extracted. With the *winmk* software (http://www.appstate.edu/~grayro/MK/winmk.htm), we obtained a normalized spectrum, which is displayed in Figure 2. By comparing the spectra of standard stars [24], the spectral type is determined to be F8V for the primary (i.e., more massive component) of this binary because the secondary is eclipsed by the primary around phase 0.0 for the W-type contact binary (see Section 4).

3. Eclipse Times and Period Analysis

From our new observations and AAVSO's data, several times of primary and secondary minima are generally determined by using the method of Kwee & van Woerden [25]. From ASAS-SN database, we downloaded 134 data types in V band

Table 2: New observed light minimum times.

JD(Hel.)	Error	Min	Band	Telescope/Source
2456629.94355	±0.00025	II	V	85-cm (NAOC)
2456629.94379	±0.00022	II	R_c	85-cm (NAOC)
2456631.98406	±0.00015	I	V	85-cm (NAOC)
2456631.98401	±0.00014	I	R_c	85-cm (NAOC)
2456634.02521	±0.00010	II	V	85-cm (NAOC)
2456634.02392	±0.00027	II	R_c	85-cm (NAOC)
2456569.20623	±0.00022	I	V	AAVSO
2456569.36322	±0.00007	II	V	AAVSO
2456573.28617	±0.00025	I	V	AAVSO
2456573.60003	±0.00011	I	V	AAVSO
2456576.42499	±0.00018	I	V	AAVSO
2456576.58236	±0.00010	II	V	AAVSO
2456579.24973	±0.00008	I	V	AAVSO
2456579.56341	±0.00007	I	V	AAVSO
2457011.76746		II	V	ASAS-SN

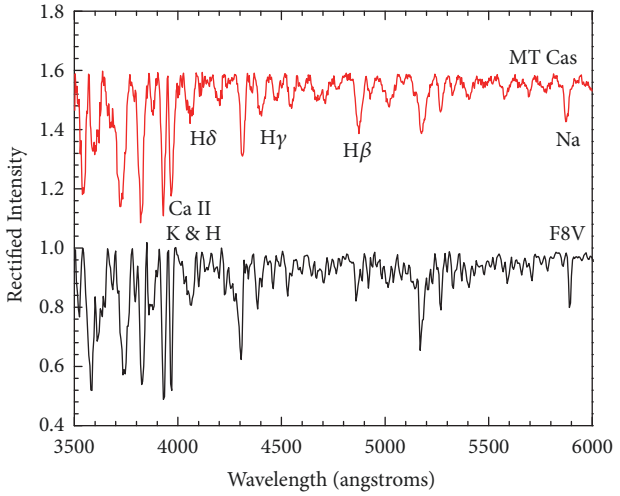

Figure 2: Spectroscopic observation for MT Cas, observed by the 2.4-m telescope at Lijiang station of YNAO on October 22, 2018.

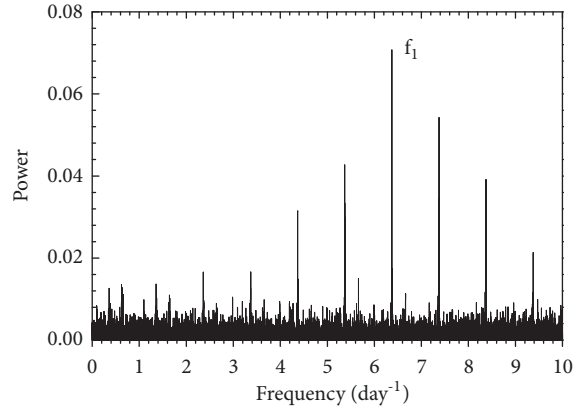

Figure 3: The power spectrum for 134 ASAS-SN data types by Fourier analysis.

for this binary. With the Period04 package [26], we obtained the power spectrum, which is shown in Figure 3. The searched frequency is $f_1 = 6.37192\text{d}^{-1}$, corresponding to 0.156937 days (i.e., half of an orbital period). The derived epoch HJD 2457010.9922 (i.e., the secondary eclipse time) a bit differs from the given rough epoch HJD 2457011.76746 from the ASAS-SN database. The individual single-color minimum timings with their errors are listed in Table 2.

In order to construct the $(O - C)$ curve (i.e., observed values minus calculated ones), we collected all available light minimum times. From the $O - C$ gateway (http://var2.astro.cz/) and TIDAK [14] (http://www.as.up.krakow.pl/minicalc/CASMT.HTM), we accumulated 10 "pg" (i.e., photographic), 21 "pe" (i.e., photoelectric), and 34 CCD measurements. Table 3 lists all those eclipsing times, whose errors are not given for 10 pg, 4 pe, and 1 CCD from literature. The standard derivations for all pe and CCD data are averaged to be 0.00137 days. For light minimum times without errors, we adopted the errors of 0.0137 for 10 pg data and 0.0014 days for 4 pe and 2 CCD ones. Therefore, the used weights depend on their errors while fitting the $(O - C)$ curve.

By using the linear ephemeris [14],

$$\text{Min.I} = \text{HJD } 2452500.086 + 0.3138789 \times E, \quad (1)$$

we compute the initial residuals, $(O - C)_i$, which are listed in Table 3 and shown in Figure 4(a). From this figure, there exists a long gap between HJD 2430024.400 [10] and HJD 2451550.2943 [27], except for three data types [12]. However, the general trend of $(O-C)_i$ may be evidently described by an

Table 3: All light minimum times for MT Cas.

JD(Hel.)	Error	Epoch	Method	Min	$(O-C)_i$ (days)	$(O-C)_f$ (days)	Ref.
2429113.517		−74508.5	pg	II	+0.0160	−0.0055	(1)
2429129.388		−74458.0	pg	I	+0.0362	+0.0147	(1)
2429144.431		−74410.0	pg	I	+0.0131	−0.0083	(1)
2429170.336		−74327.5	pg	II	+0.0231	+0.0017	(1)
2429229.342		−74139.5	pg	II	+0.0200	−0.0013	(1)
2429249.431		−74075.5	pg	II	+0.0208	−0.0004	(1)
2429464.441		−73390.5	pg	II	+0.0243	+0.0035	(1)
2429491.425		−73304.5	pg	II	+0.0148	−0.0059	(1)
2429498.493		−73282.0	pg	I	+0.0205	−0.0002	(1)
2430024.400		−71606.5	pg	II	+0.0247	+0.0050	(1)
2444901.5705		−24208.5	pe	II	−0.0004	−0.0015	(2)
2444941.5925		−24081.0	pe	I	+0.0021	+0.0010	(2)
2444955.2420		−24037.5	pe	II	−0.0021	−0.0032	(2)
2451550.2943	±0.0030	−3026.0	CCD	I	−0.0001	+0.0000	(2)
2451780.3698	±0.0021	−2293.0	CCD	I	+0.0028	+0.0029	(3)
2451807.3638	±0.0002	−2207.0	pe	I	+0.0032	+0.0033	(2)
2451924.2811	±0.0016	−1834.5	CCD	II	+0.0009	+0.0010	(4)
2452096.4442	±0.0031	−1286.0	CCD	I	+0.0019	+0.0019	(3)
2452151.3705	±0.0025	−1111.0	CCD	I	−0.0005	−0.0004	(3)
2452190.2867	±0.0016	−987.0	CCD	I	−0.0052	−0.0052	(5)
2452205.3590	±0.0031	−939.0	CCD	I	+0.0010	+0.0010	(3)
2452205.5152	±0.0016	−938.5	CCD	II	+0.0002	+0.0002	(3)
2452219.4813	±0.0028	−894.0	CCD	I	−0.0013	−0.0013	(3)
2452574.321	±0.002	236.5	CCD	II	−0.0008	−0.0008	(2)
2452684.3376	±0.0056	587.0	CCD	I	+0.0015	+0.0014	(2)
2452859.4828		1145.0	CCD	I	+0.0027	+0.0026	(3)
2452879.5725	±0.0033	1209.0	CCD	I	+0.0042	+0.0041	(2)
2453302.6749	±0.0004	2557.0	CCD	I	−0.0011	−0.0013	(2)
2453329.6671	±0.0002	2643.0	CCD	I	−0.0024	−0.0027	(2)
2453353.3663	±0.0007	2718.5	CCD	II	−0.0010	−0.0013	(2)
2453738.6533	±0.0001	3946.0	CCD	I	+0.0006	+0.0002	(2)
2453759.3698	±0.0022	4012.0	pe	I	+0.0011	+0.0007	(2)
2453767.5305	±0.0001	4038.0	CCD	I	+0.0010	+0.0006	(2)
2454205.3900	±0.0014	5433.0	pe	I	+0.0005	−0.0001	(2)
2454432.3199	±0.0003	6156.0	pe	I	−0.0035	−0.0041	(2)
2454432.4779	±0.0002	6156.5	pe	II	−0.0024	−0.0030	(2)
2454792.6557	±0.0004	7304.0	CCD	I	+0.0002	−0.0006	(2)
2455067.4622	±0.0014	8179.5	pe	II	+0.0064	+0.0055	(2)
2455074.3675	±0.0006	8201.5	pe	II	+0.0064	+0.0055	(2)
2455074.5247	±0.0004	8202.0	pe	I	+0.0067	+0.0058	(2)
2455473.3027	±0.0009	9472.5	pe	II	+0.0025	+0.0014	(2)
2455473.4600	±0.0056	9473.0	pe	I	+0.0029	+0.0018	(2)
2455473.6167	±0.0008	9473.5	pe	II	+0.0026	+0.0015	(2)
2455517.7157	±0.0003	9614.0	CCD	I	+0.0018	+0.0006	(2)
2455797.5418	±0.0087	10505.5	pe	II	+0.0055	+0.0042	(2)
2456254.7090	±0.0002	11962.0	CCD	I	+0.0092	+0.0076	(2)
2456569.2062	±0.0002	12964.0	CCD	I	+0.0006	−0.0011	(6)
2456569.3632	±0.0001	12964.5	CCD	II	+0.0006	−0.0011	(6)
2456573.2862	±0.0003	12977.0	CCD	I	+0.0001	−0.0017	(6)
2456573.6000	±0.0001	12978.0	CCD	I	+0.0001	−0.0017	(6)

Table 3: Continued.

JD(Hel.)	Error	Epoch	Method	Min	$(O-C)_i$ (days)	$(O-C)_f$ (days)	Ref.
2456576.4250	±0.0002	12987.0	CCD	I	+0.0001	−0.0017	(6)
2456576.5824	±0.0001	12987.5	CCD	II	+0.0005	−0.0013	(6)
2456579.2497	±0.0001	12996.0	CCD	I	+0.0000	−0.0018	(6)
2456579.5634	±0.0001	12997.0	CCD	I	−0.0002	−0.0019	(6)
2456629.9437	±0.0002	13157.5	CCD	II	+0.0026	+0.0008	(6)
2456631.9840	±0.0001	13164.0	CCD	I	+0.0027	+0.0009	(6)
2456634.0246	±0.0002	13170.5	CCD	II	+0.0031	+0.0013	(6)
2456950.2602	±0.0013	14178.0	pe	I	+0.0065	+0.0045	(2)
2456950.4193	±0.0015	14178.5	pe	II	+0.0086	+0.0066	(2)
2456950.5733	±0.0005	14179.0	pe	I	+0.0057	+0.0037	(2)
2457010.9918		14371.5	CCD	II	+0.0037	−0.0017	(6)
2457297.4095		15284.0	pe	I	+0.0066	+0.0044	(2)
2457322.3625	±0.0006	15363.5	pe	II	+0.0062	+0.0040	(2)
2457364.2629	±0.0004	15497.0	pe	I	+0.0039	+0.0016	(2)
2457364.4204	±0.0018	15497.5	pe	II	+0.0045	+0.0022	(2)

Ref. (1) Götz & Wenzel 1956; (2) http://www.konkoly.hu/IBVS/IBVS.html; (3) [41]; (4) [42]; (5) [43]; (6) present work.

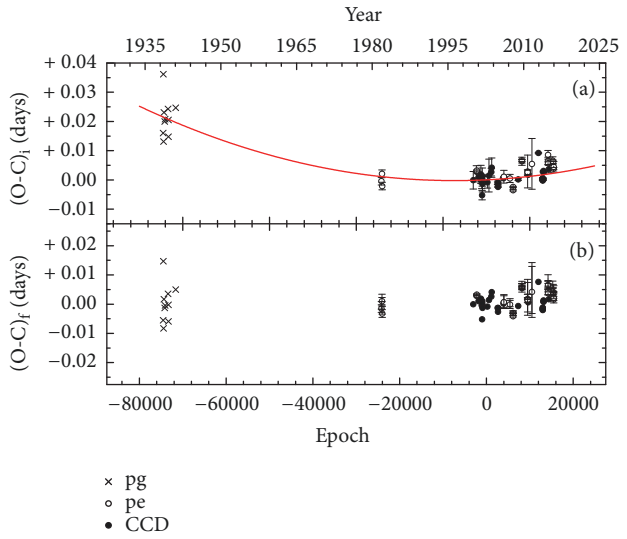

Figure 4: The $(O-C)$ curve for MT Cas. The crossing, open, and solid circles represent photographic data and photoelectric and CCD measurements, respectively. The continuous line is plotted by Eq. (2).

upward parabolic curve. A linear least-squares fitting method with weights leads to the following ephemeris:

$$\begin{aligned}\text{Min. I} = \text{HJD } 2452500.0896\,(\pm 0.0011)\\ + 0.31387820\,(\pm 0.00000002) \times E\\ + 4.82\,(\pm 0.04) \times 10^{-12} \times E^2\end{aligned} \quad (2)$$

After being removed by Eq. (2), we obtained the final residuals of $(O-C)_f$, which are listed in Table 3 and shown in Figure 4(b). If we neglected low-precision photographic data, we could find no regularity, such as sinusoidal variation, only from pe and CCD data, which can be directly seen from the right part of Figure 4(b) except for a bit scatter.

4. Modeling Light Curves

From the AAVSO and ASAS-SN databases, two additional V-band LCs for MT Cas are available and are displayed in Figure 5. Therefore three sets LCs are applied to derive the photometric elements with the updated Wilson-Devinney binary star modeling program [28, 29] (W-D program can be accessed from the site of ftp://ftp.astro.ufl.edu/pub/wilson/lcdc2015.). Kurucz's [30] stellar atmosphere model was applied. Based on the spectral type of F8V with a subtype error, we adopted a mean effective temperature for the more massive component (i.e., the primary) to be $T_p = 5750(\pm 210)$ K (the subscripts "p" and "s" refer to the primary component and the secondary one, respectively). We fixed the gravity-darkening coefficients of $g_{p,s} = 0.32$ [31] and bolometric albedo coefficients of $A_{p,s} = 0.5$ [32], which are appropriate for stars with convective envelopes. The logarithmic limb-darkening coefficients are interpolate from van Hamme's [33] tables. Other adjustable parameters are i, q, T_s, $\Omega_p = \Omega_s$, and L_s.

Due to lack of radial velocity curves, the "q-search" process is carried out by obtaining a series of tried solutions from VR_c light curves. Modeling calculations start to mode 2 (i.e., detached configuration) and always converge to mode 3 (i.e., contact one). For several fixed inclinations from 70° to 90° with a step of 5°, we first performed a series of solutions. Five computed curves for $q - i$ are shown in Figure 6(a), in which a minimum squared residual, $\Sigma(o-c)_i^2$, occurs around $q = 2.4$ and $i = 85°$. As a free parameter for the orbital inclination, we obtained the relations of $q - \Sigma$ and $q - f$ (the fill-out factor for contact binary is defined by $f = (\Omega_{in} - \Omega)/(\Omega_{in} - \Omega_{out})$, in which Ω_{in} and Ω_{out} are

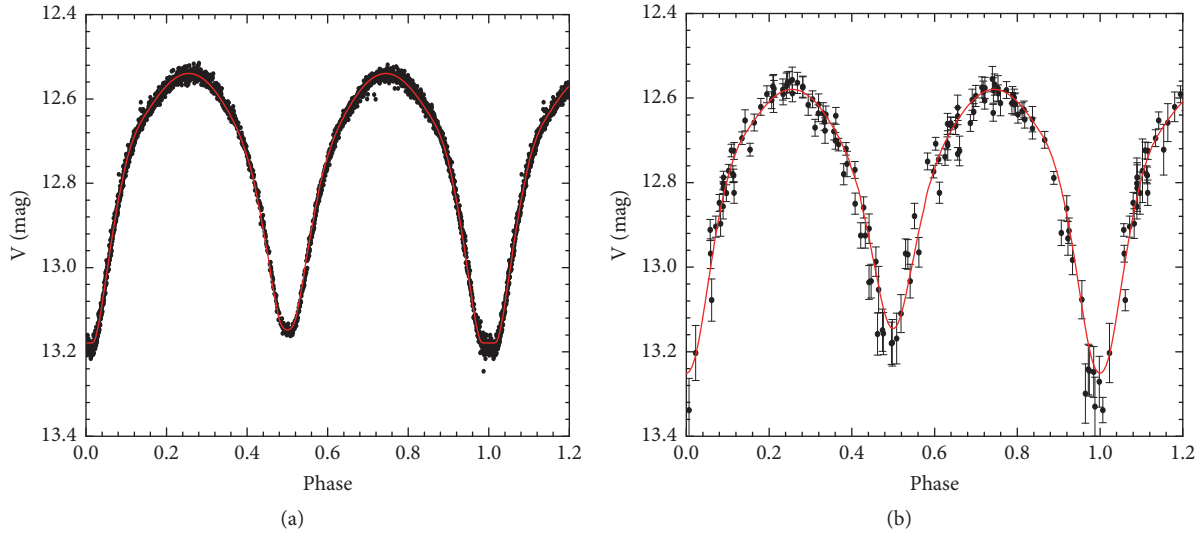

Figure 5: AAVSO's (a) and ASAS' (b) light curves. The solid lines are the theoretical LCs, which are computed by the photometric solutions.

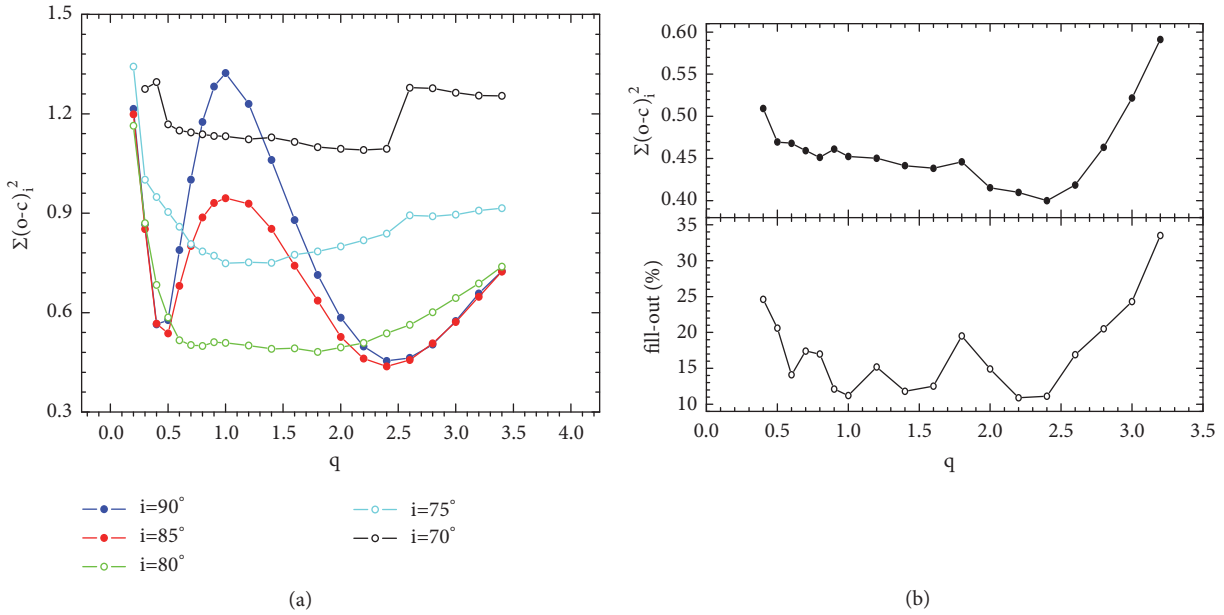

Figure 6: The relations of $q - i$ (a), $q - \Sigma$ and $q - f$ (b) derived from VR_c light curves in 2013.

inner and outer critical potentials, respectively), which are displayed in Figure 6(b). The mass-ratio of $q = 2.4$ with a minimum value of $\Sigma(o - c)_i^2$ indicates that MT Cas is a W-type contact binary (i.e., the less massive component eclipsed by the more massive component at the primary minima; see [34]). After q is considered to be a free parameter, we deduced the photometric solution, which is listed in Table 4. The calculated light curves as dotted lines are shown in Figure 1. Because VR_c LCs in 2013 cause unequal heights between both light maxima up to Max.I-Max.II~ 0.03 mag, a dark spot is added in modeling the asymmetric LCs. Assuming a cool spot on the equator of the more massive component (i.e., colatitude, $\phi = 90^\circ$), we obtained the final photometric elements, which are given in Table 4, including other three parameters of spot (i.e., longitude θ, angular radius γ, and temperature factor T_{spot}/T_p). The mass ratio and fill-out factor for MT Cas are $q = 2.365(\pm 0.005)$ and $f = 16.6(\pm 1.2)\%$, respectively. The corresponding theoretical light curves as solid lines are plotted in Figure 1. The O'Connell effect for this binary can be attributed the activity of stellar spot. Its area is up to 1.7% of the area of the more massive component. Therefore, the spotted solution is accepted to be the final solution due to its small value of $\Sigma(o - c)_i^2 = 0.2223$. Additionally, we analyzed AAVSO's and ASAS' LCs, respectively. The derived photometric solutions are given in Table 4. The mass ratio and fill-out factor almost agree with the previous result from our

Table 4: Photometric solutions for MT Cas.

Parameters	LCs in 2013		LC of AAVSO	LC of ASAS
	No Spot	With Spot	(2878 data types)	(134 data types)
$i(^\circ)$	84.7 ± 0.3	85.2 ± 0.3	83.6 ± 0.1	80.3 ± 0.2
$q = M_p/M_s$	2.370 ± 0.002	2.365 ± 0.005	2.487 ± 0.025	2.415 ± 0.013
$T_p(K)$	5750 ± 210		5750 ± 210	
X_p, Y_p	0.650, 0.207		0.650, 0.207	
x_{sV}, y_{sV}	0.774, 0.232		0.774, 0.232	
x_{sR}, y_{sR}	0.694, 0.251		0.694, 0.251	
$T_s(\mathrm{K})^a$	6010^{+145}_{-238}	6026^{+231}_{-249}	5966^{+232}_{-232}	6080^{+236}_{-137}
X_s, Y_s	0.649, 0.221	0.649, 0.222	0.649, 0.219	0.648, 0.225
x_{sV}, y_{sV}	0.746, 0.260	0.745, 0.261	0.749, 0.256	0.742, 0.265
x_{sR}, y_{sR}	0.675, 0.271	0.674, 0.271	–	
$\Omega_p = \Omega_s$	5.678 ± 0.006	5.660 ± 0.007	5.857 ± 0.004	5.767 ± 0.031
$L_s/(L_p + L_s)_V$	0.3602 ± 0.0006	0.3641 ± 0.0006	0.3422 ± 0.0002	0.3681 ± 0.0049
$L_s/(L_p + L_s)_R$	0.3544 ± 0.0005	0.3559 ± 0.0005	–	
r_p(pole)	0.4342 ± 0.0013	0.4373 ± 0.0012	0.4375 ± 0.0005	0.4345 ± 0.0019
r_p(side)	0.4643 ± 0.0018	0.4683 ± 0.0016	0.4681 ± 0.0006	0.4644 ± 0.0025
r_p(back)	0.4937 ± 0.0024	0.4988 ± 0.0021	0.4868 ± 0.0008	0.4931 ± 0.0029
r_s(pole)	0.2932 ± 0.0016	0.2946 ± 0.0015	0.2884 ± 0.0005	0.2900 ± 0.0018
r_s(side)	0.3067 ± 0.0019	0.3083 ± 0.0018	0.3015 ± 0.0006	0.3030 ± 0.0022
r_s(back)	0.3438 ± 0.0032	0.3469 ± 0.0031	0.3380 ± 0.0009	0.3390 ± 0.0023
θ(arc)	–	1.61 ± 0.07	–	
γ(arc)	–	0.26 ± 0.04	–	
T_{spot}/T_p	–	0.85 ± 0.05	–	
$\Sigma(o-c)_i^2$	0.3777	0.2223	0.2762	1.1616
$f(\%)$	14.8 ± 1.1	16.6 ± 1.2	11.5 ± 0.6	10.2 ± 0.5

Note. [a]The uncertainty of T_s is determined from the input error for T_p.

VR_c light curves. The calculated LCs are plotted as continuous lines in Figure 6. Their mass-ratios approximate to the result of the photometric solution with a cool spot.

5. Results and Discussions

Up to now no spectroscopic elements have been published, and the absolute parameters of this binary cannot be directly determined. Assuming the spectral type of F8V with a subtype uncertainty, the mass of the primary was roughly estimated to be $M_p = 1.19(\pm0.07)\ \mathrm{M}_\odot$ [35]. Using the mass ratio and orbital period, the separation between components and the mass of the secondary are estimated to be $a = 2.32(\pm0.05)\ \mathrm{R}_\odot$ and $M_s = 0.50(\pm0.03)\ \mathrm{M}_\odot$, respectively. Other absolute parameters for MT Cas are as follows: $R_p = 1.08(\pm0.05)\ \mathrm{R}_\odot$, $R_s = 0.73(\pm0.04)\ \mathrm{R}_\odot$, $L_p = 1.15(\pm0.11)\ \mathrm{R}_\odot$, and $L_s = 0.63(\pm0.07)\ \mathrm{R}_\odot$.

The mass-luminosity diagram is displayed in Figure 7, in which the zero-age main sequence (ZAMS) and the terminal-age main sequence (TAMS) are constructed by the binary-star evolution code [36]. The W-type low-temperature contact binaries (LTCBs; see [3]) are plotted as black open and filled circles. From this figure, the primary component of MT Cas is close to the TAMS line, implying that it is a normal main-sequence star. Meanwhile, the secondary component lies above the TAMS line, indicating that it may be a small helium star in an advanced evolutionary stage [4].

From Eq. (2), the orbital period of MT Cas may be undergoing a secular increase at a rate of $dP/dt = +1.04(\pm0.09) \times 10^{-8}$ d yr^{-1}. This case occurs in other weak-contact binaries, which are listed in Table 5. Therefore, the period increase rate for MT Cas may be a small value for this kind of binaries. The long-term period increases can be generally interpreted by mass transfer from the less massive component to the more massive one. Under conserved mass transfer assumption, the mass transfer rate can be computed by the following formula [37]:

$$\frac{\dot{P}}{P} = 3\left(\frac{M_p}{M_s} - 1\right)\frac{\dot{M}_p}{M_p}. \tag{3}$$

Inserting the values of $\dot{P}$, P, M_p, and M_s into Eq. (3), the mass transfer rate is estimated to be $\dot{M}_p = +1.04(\pm0.09) \times 10^{-8}\mathrm{M}_\odot\ \mathrm{yr}^{-1}$. With the period increasing, the separation between two components will increase. Meanwhile, mass transfer from the secondary one to the primary one also causes the mass ratio to decrease. This may result in the inner and outer Roche lobes shrinking, which will cause the fill-out factor to decrease. Finally, the weak-contact configuration

Table 5: Several weak-contact binaries with secular period increasing.

Star	Spectral type	Period (day)	q	dP/dt ($\times 10^{-7}$d yr^{-1})	f (%)	Ref.
44i Boo	K2V	0.26782	0.487	+1.49	5.0	(1)(2)
CW Cas	G8V	0.31886	0.448	−0.34	6.5	(3)
BE Cep	–	0.42439	0.427	−0.48	6.9	(4)
DD Com	–	0.26921	0.271	+3.4	8.8	(5)
AD Cnc	K0V	0.28274	0.770	+4.94	8.3	(6)
XY Leo	K2V	0.28410	0.610	+0.27	6.7	(7)
MT Cas	F8V	0.31388	0.423[a]	+0.11	16.6	(8)

Note. [a]The mass ratio is flipping, i.e., 1/2.365.
References: (1) [44]; (2) [45]; (3) [46]; (4) [47]; (5) [48]; (6) [49]; (7) [50]; (8) present paper.

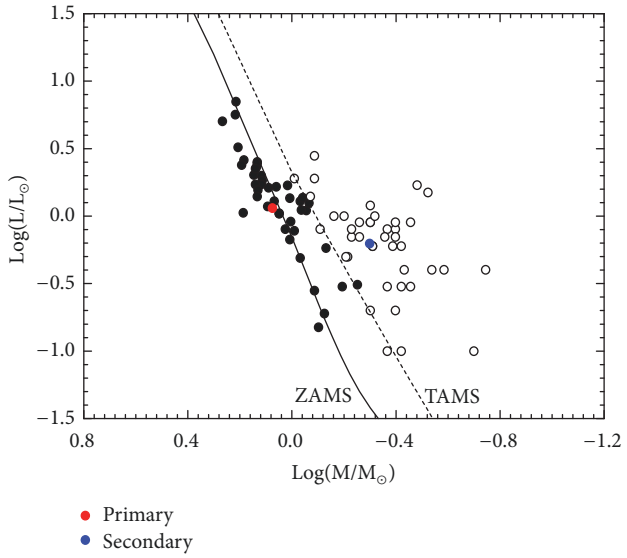

Figure 7: The mass-luminosity diagram for MT Cas. The filled and open circles represent the primary and secondary components for the W-type LTCBs [3].

may be broken. Therefore, MT Cas may evolve into a broken-contact configuration, as predicted by TRO theory [3, 38–40]. In the future, it necessitates to obtain high-precision photometry and spectroscopy to identify the orbital period variations and to determine its absolute parameters.

Data Availability

The data used to support the findings of this study are included within the article.

Conflicts of Interest

The authors declare that they have no conflicts of interest.

Acknowledgments

This research is partly supported by the National Natural Science Foundation of China (grants Nos. 11873003 & 11473009), Natural Science Research Project of the Educational Department of Anhui Province (grant No. KJ2017A850), and the Outstanding Young Talents Program (grant No. gxyq2018161) of the Educational Department of Anhui Province. New observations of MT Cas were obtained by using the 60/85-cm telescopes at the Xinglong Station of NAOC and 2.4-m telescope at the Lijiang Station of YNAO.

Supplementary Materials

Table 1: CCD photometric observations in V and R_c bands. *(Supplementary Materials)*

References

[1] L. B. Lucy, "The structure of contact binaries," *Astrophysical Journal*, vol. 151, p. 1123, 1968.
[2] L. B. Lucy, "The Light Curves of W Ursae Majoris Stars," *Astrophysical Journal*, vol. 153, p. 877, 1968.
[3] K. Yakut and P. P. Eggleton, "Evolution of close binary systems," *The Astrophysical Journal*, vol. 629, no. 2, pp. 1055–1074, 2005.
[4] K. stępień, "Evolutionary status of late-type contact binaries," *Acta Astronomica*, vol. 56, p. 199, 2006.
[5] L.-F. Li, F.-H. Zhang, Z. Han, and D.-K. Jang, "Formation and evolution of w ursae majoris contact binaries," *The Astrophysical Journal*, vol. 662, no. 1, p. 596, 2007.
[6] J. H. Applegate, "A mechanism for orbital period modulation in close binaries," *Astrophysical Journal*, vol. 385, pp. 621–629, 1992.
[7] J. B. Irwin, "The determination of a light-time orbit," *The Astrophysical Journal*, vol. 116, p. 211, 1952.
[8] S.-B. Qian, J.-J. Wang, L.-Y. Zhu et al., "Optical flares and a long-lived dark spot on a cool shallow contact binary," *The Astrophysical Journal Supplement Series*, vol. 212, no. 1, p. 4, 2014.
[9] R. Tylenda, M. Hajduk, T. Kamiński et al., "V1309 Scorpii: merger of a contact binary," *Astronomy & Astrophysics*, vol. 528, Article ID A114, p. 10, 2011.
[10] W. Götz and W. Wenzel, "Die veraenderlichen Sterne der nordlichen Milstrasse. Teil VIII," *Veroeff. Sternwarte Sonneberg*, vol. 2, pp. 279–366, 1956.
[11] O. Y. Malkov, E. Oblak, E. A. Snegireva, and J. Torra, "A catalogue of eclipsing variables," *Astronomy & Astrophysics* , vol. 446, no. 2, pp. 785–789, 2006.
[12] M. Hoffmann, "MT Cassiopeiae, Another Contact Binary with Complete Eclipses," Information Bulltin on Variable Stars, 2063, 1, 1982.

[13] T. Pribulla, J. M. Kreiner, and J. Tremko, "Catalogue of the field contact binary stars," *Contributions of the Astronomical Observatory Skalnaté Pleso*, vol. 33, no. 1, pp. 38–70, 2003.

[14] J. M. Kreiner, "Up-to-date linear elements of eclipsing binaries," *Acta Astronomica*, vol. 54, pp. 207–210, 2004.

[15] T. Jayasinghe, K. Z. Stanek, C. S. Kochanek et al., "The ASAS-SN Catalog of Variable Stars II: Uniform Classification of 412,000 Known Variables," 2018, http://adsabs.harvard.edu/abs/2018arXiv180907329J.

[16] A.-Y. Zhou, X.-J. Jiang, Y.-P. Zhang, and J.-Y. Wei, "MiCPhot: a prime-focus multicolor CCD photometer on the 85-cm telescope," *Research in Astronomy and Astrophysics*, vol. 9, no. 3, p. 349, 2009.

[17] E. F. Milone, "The peculiar binary RT Lacertae," *Astronomical Journal*, vol. 73, pp. 708–711, 1968.

[18] T. J. Davidge and E. F. Milone, "A study of the O'Connell effect in the light curves of eclipsing binaries," *Astrophysical Journal*, vol. 55, pp. 571–584, 1984.

[19] G. Kaszás, J. Vinkó, K. Szatmáry et al., "Period variation and surface activity of the contact binary VW Cephei," *Astronomy & Astrophysics* , vol. 331, no. 1, pp. 231–243, 1998.

[20] H.-F. Dai, Y.-G. Yang, and X.-G. Yin, "A photometric study of the W UMa-type binary DF Canum Venaticorum," *New Astron*, vol. 16, no. 3, pp. 173–176, 2011.

[21] Y.-G. Yang, H.-F. Dai, H.-Y. Yuan, and X.-L. Zhang, "Photometric studies for two contact binaries: V532 monocerotis and GU orionis," *Publications of the Astronomical Society of Japan*, vol. 69, no. 4, Article ID 69, 2017.

[22] Y.-G. Yang, S.-B. Qian, L.-Y. Zhang et al., "Deep, low mass ratio overcontact binary systems. XIII. DZ piscium with intrinsic light variability," *The Astronomical Journal*, vol. 146, no. 2, p. 35, 2013.

[23] Y.-F. Fan, J.-M. Bai, J.-J. Zhang et al., "Rapid instrument exchanging system for the Cassegrain focus of the Lijiang 2.4-m Telescope*," *Astronomy and Astrophysics*, vol. 15, no. 6, p. 918, 2015.

[24] A. J. Pickles, "A stellar spectral flux library: 1150–25000 Å," *Publications of the Astronomical Society of the Pacific*, vol. 110, no. 749, p. 863, 1998.

[25] K. K. Kwee and H. van Woerden, "A method for computing accurately the epoch of minimum of an eclipsing variable," *Bulletin of the Astronomical Institutes of the Netherlands*, vol. 12, p. 327, 1956.

[26] P. Lenz and M. Breger, "Period04 user guide," *Communications in Asteroseismology*, vol. 146, pp. 53–136, 2005.

[27] M. Zejda, "CCD Times of Minima of Faint Eclipsing Binaries in 2000," Information Bulltin on Variable Stars, 5287, 1, 2002.

[28] R. E. Wilson and E. J. Devinney, "Realization of Accurate Close-Binary Light Curves: Application to MR Cygni," *Astrophysical Journal*, vol. 166, p. 605, 1971.

[29] R. E. Wilson, "Accuracy and efficiency in the binary star reflection effect," *The Astrophysical Journal*, vol. 356, pp. 613–622, 1990.

[30] R. L. Kurucz, "Peculiar versus normal phenomena in a-type and related stars," in *Proceedings of the International Astronomical Union, Colloquium No. 138*, vol. 44, p. 87, Astronomical Society of the Pacific, San Francisco, Calif, USA, 1993.

[31] L. B. Lucy, "Gravity-darkening for stars with convective envelopes," *Zeitschrift für Astrophysik*, vol. 65, p. 89, 1967.

[32] S. M. Rucinski, "The W UMa-type systems as contact binaries. I. Two methods of geometrical elements determination. Degree of contact," *Acta Astronomica*, vol. 23, p. 79, 1973.

[33] W. van Hamme, "New limb-darkening coefficients for modeling binary star light curves," *Astronomical Journal*, vol. 106, no. 5, pp. 2096–2117, 1993.

[34] L. Binnendijk, "The orbital elements of W Ursae Majoris systems," *Vistas in Astronomy*, vol. 12, pp. 217–256, 1970.

[35] A. N. Cox, *Allen's Astrophysical Quantities*, Springer, New York, NY, USA, 4th edition, 2000.

[36] J. R. Hurley, C. A. Tout, and O. R. Plos, "Evolution of binary stars and the effect of tides on binary populations," *Monthly Notices of the Royal Astronomical Society*, vol. 329, no. 4, pp. 897–928, 2002.

[37] M. Singh and U. S. Chaubey, "Mass loss from wolf-rayet stars," *Astrophysics and Space Science*, vol. 124, no. 2, pp. 389–396, 1986.

[38] L. B. Lucy, "W Ursae Majoris systems with marginal contact," *The Astrophysical Journal* , vol. 205, pp. 208–216, 1976.

[39] B. P. Flannery, "A cyclic thermal instability in contact binary stars," *The Astrophysical Journal* , vol. 205, pp. 217–225, 1976.

[40] J. A. Robertson and P. P. Eggleton, "The evolution of W Ursae Majoris systems," *Monthly Notices of the Royal Astronomical Society*, vol. 179, no. 3, pp. 359–375, 1977.

[41] L. Brát, M. Zejda, and P. Svoboda, "B.R.N.O. Contributions #34," *Open European Journal on Variable Stars*, vol. 74, no. 1, p. 1, 2007.

[42] R. Diethelm, "157. List of minima of eclipsing binaries," Tech. Rep., The group of eclipsing binary observers of the Swiss Astronomical Society (BBSAG) Bulletins, BBSAG Bull., 124, 1, 2001.

[43] E. Blättler, "159. List of minima of eclipsing binaries," Tech. Rep., The group of eclipsing binary observers of the Swiss Astronomical Society (BBSAG) Bulletins, BBSAG Bull., 126, 1, 2001.

[44] W. Lu, S. M. Rucinski, and W. Ogłoza, "Radial Velocity Studies of Close Binary Stars. IV.*," *The Astronomical Journal*, vol. 122, no. 1, p. 402, 2001.

[45] G. Hill, W. A. Fisher, and D. Holmgren, "Studies of late-type binaries. I. The physical parameters of 44i Bootis ABC," *Astronomy and Astrophysics*, vol. 211, pp. 81–98, 1989.

[46] T.-Y. Jiang, L.-F. Li, Z.-W. Han, and D.-K. Jiang, "Photometric investigation and possible light-time effect in the orbital period of a marginal contact system, CW cassiopeiae," *Publications of the Astronomical Society of Japan*, vol. 62, no. 2, pp. 457–465, 2010.

[47] H.-F. Dai and Y.-G. Yang, "A comprehensive photometric study of the marginal-contact binary BE Cephei," *New Astron*, vol. 17, no. 3, pp. 347–352, 2012.

[48] L. Zhu, S.-B. Qian, Z. Mikulášek et al., "Photometric study of the very short period shallow contact binary DD comae berenices," *The Astronomical Journal*, vol. 140, no. 1, Article ID 215, 2010.

[49] S.-B. Qian, J.-Z. Yuan, B. Soonthornthum et al., "AD cancri: a shallow contact solar-type eclipsing binary and evidence for a dwarf third component and a 16 year magnetic cycle," *The Astrophysical Journal*, vol. 671, no. 1, p. 811, 2007.

[50] K. Yakut, C. İbanoğlu, B. Kalomeni, and Ö. L. Değirmenci, "New light curve analysis and period changes of the overcontact binary XY Leonis," *Astronomy and Astrophysics*, vol. 401, pp. 1095–1100, 2003.